Limnol. Oceanogr., 55(6), 2010, 2366–2380

doi:10.4319/lo.2010.55.6.2366

Transport and consumption of oxygen and methane in different habitats of the Håkon Mosby Mud Volcano (HMMV)

J. Felden,[a,*] F. Wenzhöfer,[a,c] T. Feseker,[b] and A. Boetius[a,c]

[a] Max Planck Institute for Marine Microbiology, Bremen, Germany
[b] Leibniz Institute of Marine Sciences at the Christian-Albrechts Universität zu Kiel (IFM-GEOMAR), Germany
[c] Alfred Wegener Institute for Polar and Marine Research, Bremerhaven, Germany

Abstract

The Håkon Mosby Mud Volcano is a highly active methane seep hosting different chemosynthetic communities such as thiotrophic bacterial mats and siboglinid tubeworm assemblages. This study focuses on in situ measurements of methane fluxes to and from these different habitats, in comparison to benthic methane and oxygen consumption rates. By quantifying in situ oxygen, methane, and sulfide fluxes in different habitats, a spatial budget covering areas of 10–1000-m diameter was established. The range of dissolved methane efflux (770–2 mmol m^{-2} d^{-1}) from the center to the outer rim was associated with a decrease in temperature gradients from 46°C m^{-1} to < 1°C m^{-1}, indicating that spatial variations in fluid flow control the distribution of benthic habitats and activities. Accordingly, total oxygen uptake (TOU) varied between the different habitats by one order of magnitude from 15 mmol m^{-2} d^{-1} to 161 mmol m^{-2} d^{-1}. High fluid flow rates appeared to suppress benthic activities by limiting the availability of electron acceptors. Accordingly, the highest TOU was associated with the lowest fluid flow and methane efflux. This was most likely due to the aerobic oxidation of methane, which may be more relevant as a sink for methane as previously considered in submarine ecosystems.

Active submarine mud volcanoes (MVs) are found worldwide at convergent and passive continental margins (Dimitrov 2002). They are characterized by fluid and gas outflows fueling a variety of cold seep communities, and are often associated with the occurrence of gas hydrates. The total number of deep-sea MVs is estimated to be in the range of 10^3–10^5 with a release of 5–20 Tg methane yr^{-1} of which an unknown fraction may also escape to the atmosphere (Kopf 2002; Milkov et al. 2003; Kvenvolden and Rogers 2005).

In cold seep ecosystems such as those associated with mud volcanism, the chemical energy in hydrocarbons emitted as fluids and gases is used as energy source for diverse chemosynthetic communities (Olu et al. 1997; Olu-Le Roy et al. 2004; Jørgensen and Boetius 2007). The flux of methane to the seafloor depends mostly on geological and physical processes in the subsurface seabed, but emission and consumption rates are considerably influenced by biological activities. Benthic oxygen and sulfate consumption are often one to two orders of magnitude higher at cold seeps compared to nonseep seafloor. However, oxygen and sulfate can be rapidly depleted in the upper millimeters or centimeters, respectively, of cold seep sediments (Treude et al. 2003; de Beer et al. 2006; Sommer et al. 2006), and some methane may pass the benthic filter against methane (Niemann et al. 2006). Although benthic microbial assemblages oxidize a significant fraction of the subsurface hydrocarbon flux, most cold seeps emit methane and other hydrocarbons into the water column either as free gas or dissolved. Unfortunately, very few quantitative estimates of the balance between methane emission and consumption by aerobic and anaerobic oxidation of methane and other hydrocarbons are available today (Niemann et al. 2006; Sommer et al. 2006; Reeburgh 2007). This is due to the lack of appropriate in situ technologies to quantify benthic fluxes, fluid flow, and biogeochemical processes together in space and time. Another challenge to process studies at mud volcanoes is the complex, dynamic interplay of physical, chemical, and biological processes shaping the mud volcano ecosystem.

For the oxidation of methane in marine settings, two main pathways have been identified: the aerobic oxidation (MOx) with oxygen performed by methanotrophic bacteria, and the anaerobic oxidation of methane (AOM) with sulfate mediated by methanotrophic archaea associated with sulfate-reducing bacteria (Knittel and Boetius 2009). Sulfide and carbonate are the end products of AOM coupled to sulfate reduction (SR; Boetius et al. 2000). Sulfide produced by AOM is the main electron donor for sulfide-oxidizing bacteria, including free-living ones such as the giant mat-forming thiotrophs, and endosymbionts of siboglinid tubeworms and several taxa of bivalves (Olu et al. 1997; Cordes et al. 2003; Teske and Nelson 2006). The presence of these chemosynthetic organisms at the seafloor is, therefore, used as an indicator of active AOM and SR microbial communities in the underlying seabed, fueled by high methane fluxes (Treude et al. 2003; Niemann et al. 2006).

Different types of methane-dependent communities occur at the Håkon Mosby Mud Volcano (HMMV), located northwest of Norway on the Barents Sea slope (72°N, 14°44′E) at a water depth of 1250 m (Milkov et al. 2004; de Beer et al. 2006; Niemann et al. 2006). The flat central area is populated by aerobic methanotrophs (Lösekann et al. 2007). At the border of the center, two types of thiotrophic bacterial mats occur (de Beer et al.

* Corresponding author: jfelden@mpi-bremen.de

2006; Niemann et al. 2006; Jerosch et al. 2007), and dense accumulations of siboglinid tubeworms populate the outer hummocky rim of the mud volcano above subsurface gas hydrates (Niemann et al. 2006; Jerosch et al. 2007). All habitats are methane-rich, but have been found to differ substantially in fluid flow velocity and sulfide production rates (de Beer et al. 2006).

The HMMV represents an ideal natural laboratory to investigate the relationships among fluid flow, methane flux, and benthic activity. Previous biogeochemical studies showed a strong coupling of AOM to SR, a repression of the microbial filter for methane by high fluid flow rates (Niemann et al. 2006), and the importance of advective fluid flow compared to mud flow for temperature gradient variability in the sediment (Feseker et al. 2008). A first attempt to budget the methane consumption and emission of the HMMV was based on a few first in situ measurements (Niemann et al. 2006), and was considering only focused methane emission, based on visual observations of gas bubble streams (Sauter et al. 2006). Methane in the form of gas bubbles is hardly accessible to microbial communities, and diffuse methane efflux may be as relevant as gaseous efflux in mud volcano systems. However, so far, only a few in situ quantifications of diffuse methane emission rates are available (Torres et al. 2002; Sommer et al. 2006, 2009).

Here we combined data from six different cruises between 2001 and 2009 to investigate spatial variations of biogeochemical processes within and between the different HMMV habitats. We investigated for the first time diffuse methane efflux and total oxygen uptake (TOU) for all HMMV habitats. Differences in total and diffusive oxygen uptake, assigned to faunal respiration (Glud 2008), were used to investigate the faunal contribution to the benthic oxygen budget. Furthermore, we inquired not only the relation between diffusive and total oxygen consumption, but also between temperature gradients, oxygen, sulfide, and methane fluxes. Based on these data, the efficiency of the benthic biological filter against methane and sulfide was estimated and compared to other cold seep systems.

Methods

Site description—Based on previous studies (Niemann et al. 2006; Jerosch et al. 2007; Lichtschlag et al. 2010) and on visual investigations, four habitats were identified and chosen for repeated sampling and in situ measurements: (I) the mud volcano center, comprising a northern zone of ~ 100-m diameter with highly disturbed seabed, surrounded by an apparently older mud flow with a smooth surface, (II) the adjacent *Beggiatoa* mats, (III) a transition zone marked by patchy bacterial mats of gray color, and (IV) dense assemblages of siboglinid tubeworms occupying the hummocky outer zone of the HMMV (Figs. 1, 2). The center of the HMMV was previously characterized by high temperature gradients, methane emission, and mud extrusion, and the absence of sulfide production and chemosynthetic macrofauna (de Beer et al. 2006; Niemann et al. 2006). In this study, differences in seafloor morphology and in situ temperature measurements have led to a further distinction in a 'hot' and 'warm' area. Adjacent to the active center, dense *Beggiatoa* mats covered large parts of the flat seafloor characterized by high fluid flow, gassy sediments, and high sulfide flux. Another bacterial mat type with a grayish color was found above gas-saturated sediments in the transition zone toward the hummocky area surrounding the center. These mats were previously characterized by the absence of fluid flow but associated with high sulfide production in the sediments (de Beer et al. 2006; Lichtschlag et al. 2010). The hummocky zone surrounding the HMMV is inhabited by two siboglinid tubeworm species that can reach high biomasses of 1–2 kg wet weight m^{-2} (Smirnov 2000; Milkov et al. 2004; Niemann et al. 2006). These tubeworms irrigate the seafloor and push the anoxic zone into deeper sediment strata (Lösekann et al. 2008).

Sampling—Repeated sediment sampling and measurements were performed in four different HMMV habitats during six cruises: HMMV (R/V *L'Atalante*, 2001), ARK XIX-3b (R/V *Polarstern*, 2003), AWI-ROV (R/V *L'Atalante*, 2005), Viking (R/V *Pourquoi pas*, 2006), ARK XXII-1b (R/V *Polarstern*, 2007), and ARK XXIV-2 (R/V *Polarstern*, 2009). Targeted sampling, precise positioning, and operation of the in situ tools at the seafloor were performed with the remotely operated vehicles (ROVs) *Victor 6000* (IFREMER) and *Quest4000* (MARUM). Sampling locations, sample labels, and all performed measurements are summarized in Table 1 and are available in the PANGAEA database (http://www.pangaea.de).

The patchy colonization of chemosynthetic organisms (e.g., tubeworms, thiotrophic bacteria) at the seafloor creates mosaic-like distribution patterns of decimeter to meter scale in each habitat. Therefore, within most habitats, measurements were carried out on patches covered with characteristic benthic assemblages and on adjacent patches lacking these. For example, measurements in the *Beggiatoa* mat habitat were performed on sediment densely covered by bacteria and additionally 'next to' the bacterial mat, where no mat was observed at the seafloor but where the sediment was still influenced by seepage.

Sediment samples from the uppermost sediment horizons (top 20–30 cm) were taken either with a video-guided multicoring device (MUC) or with push-cores (PCs) collected with the manipulator of the ROV. After recovery, the PC and MUC tubes were transferred to a cold room that was cooled to in situ temperature (0°C). The HMMV sediment was highly gas-saturated, and outgassing during retrieval of the samples often caused disturbance of the bacterial mats. Therefore, respective cores were stored for 1–2 d at in situ temperature to reestablish bacterial mats and geochemical gradients, as indicated by oxygen, sulfide, and pH microsensor measurements performed directly after core retrieval and after 36 h (de Beer et al. 2006). Afterwards, the cores were vertically subsampled with small subcore tubes (diameter = 26 mm).

To access sediment depths below 30 cm, a gravity corer (GC) was equipped with a *POSIDONIA* (Ixsea SAS) positioning system for targeted sampling of the same habitats. Sediments from the GC were subsampled with

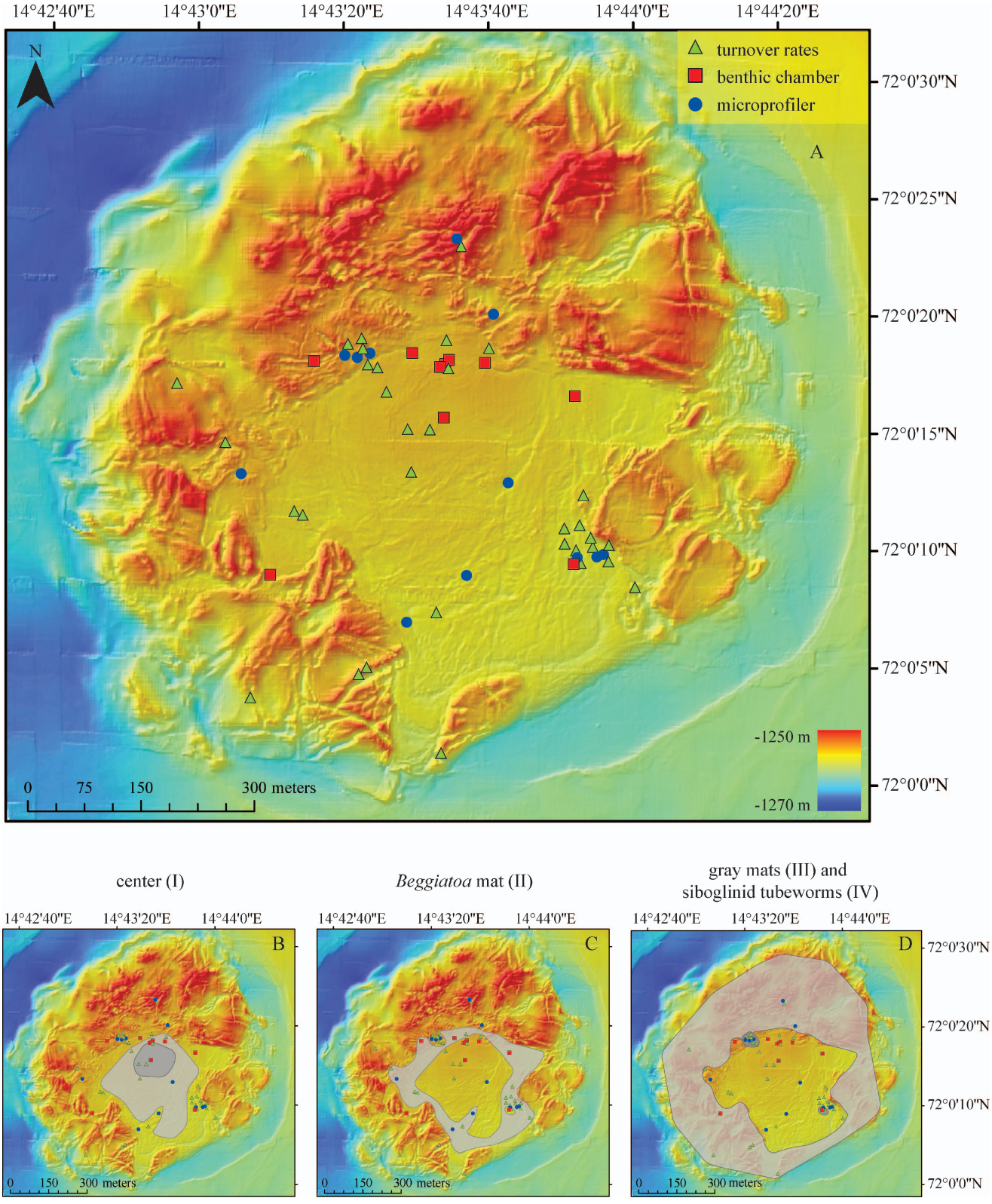

Fig. 1. (A) Bathymetric map of the HMMV (generated during ARK XIX/3b by IFREMER, Brest; Foucher et al. 2009) with the positions of all sampling stations and in situ measurements. The sediment samples for sulfate and methane turnover rates are displayed as green triangles. Total oxygen uptake measurements with the benthic chamber are shown as red squares, and the blue circles illustrate previous microprofiler measurements of the DOU (de Beer et al. 2006; Lichtschlag et al. 2010). (B–D) show the approximate dimensions of the different habitats (in gray) in relation to the sampling and in situ measurement locations. (B) The black circle marks the area characterized by a disturbed sediments and high temperature gradients. The blue circles in (D) indicate the gray mat sites sampled here.

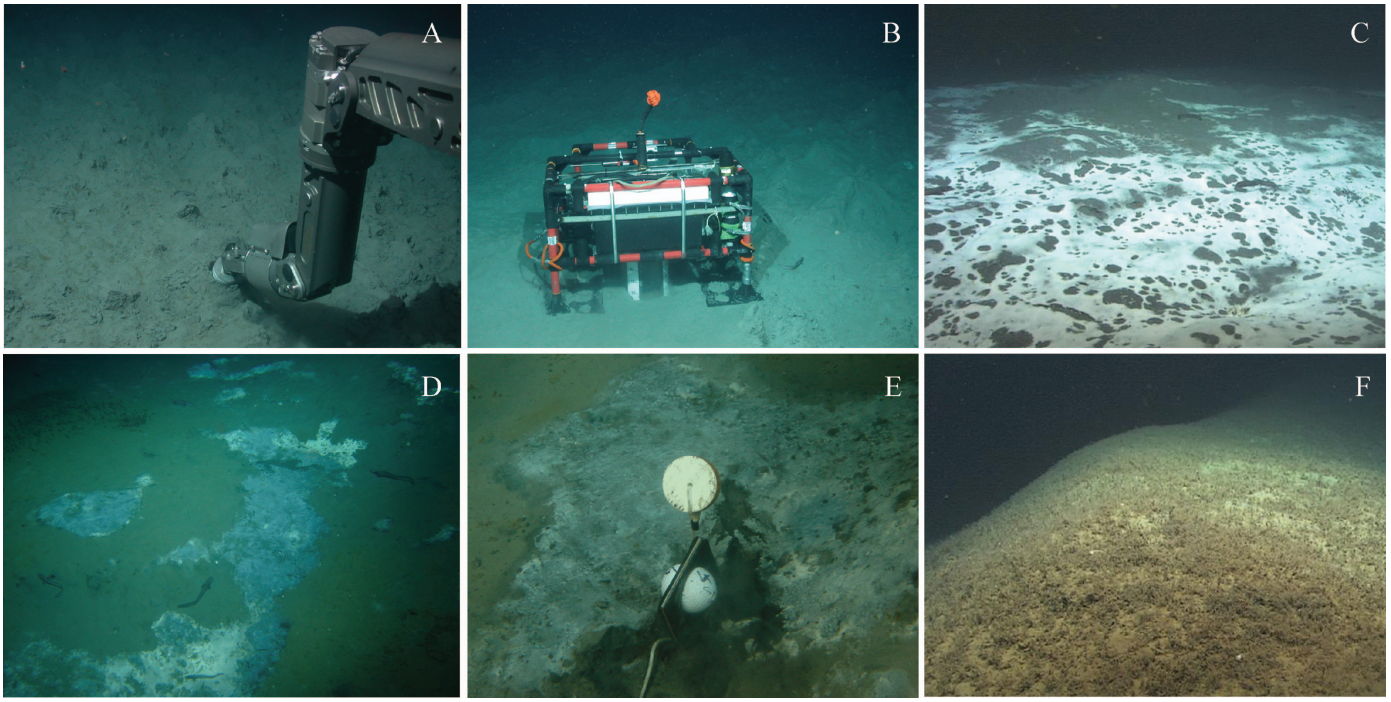

Fig. 2. Different habitats of the HMMV. (A) push core sampling in the center where the highest temperature gradients occur; (B) the benthic chamber is deployed on a smooth mudflow of the center; (C) *Beggiatoa* mats; (D) gray mats; (E) gray mat close-up with temperature probe; (F) siboglinid tubeworm habitat. All pictures are copyright of MARUM, except (D) and (E) which are copyright IFREMER.

small glass tubes (60-mm length, 10-mm diameter) immediately after the core recovery.

Methane oxidation and sulfate reduction rates—Sediment cores for measurements of methane oxidation (MOx and AOM) and SR were subsampled on board with two to four replicates per sample station. The rates were measured according to Treude et al. (2003). Either 25-μL $^{14}CH_4$ (dissolved in water, 2.5 kBq) or 5–10-μL carrier-free $^{35}SO_4^{2-}$ (dissolved in water, 50 kBq) were injected in 1-cm intervals into the subcores (whole core injection method; Jørgensen 1978). The sediment was incubated in the dark at in situ temperature for 12–48 h (PC, MUC). After the incubation, all sediment cores were cut into 1–2 cm sections. Each section was fixed in 25 mL NaOH (2.5%, w/v) or in 20 mL zinc acetate solution (20%, w/v) for methane oxidation and sulfate reduction rate measurements, respectively. Subsamples from the gravity cores were treated the same way, by either injecting 25 μL $^{14}CH_4$ (2.5 kBq) or 5–10-μL carrier-free $^{35}SO_4^{2-}$ (50 kBq) into the glass tubes. These sediments were incubated for 36 h and then preserved as described for the subcore sections. In the home laboratory, sulfate and methane consumption were quantified according to Kallmeyer et al. (2004) and Treude et al. (2003), respectively. The radioactivity of the labeled constituents was determined by scintillation counting. The substrate concentrations (methane, sulfate) were measured by gas chromatography (5890A; Hewlett Packard) and anion exchange chromatography (Waters I.C.-Pak™ anion column 50 × 4.6 mm; Waters 430 conductivity detector), respectively.

Methane turnover rates (MOx and AOM) were calculated according to the following equation:

$$\text{methane oxidation} = \frac{^{14}CO_2}{(^{14}CH_4 + ^{14}CO_2)} \times \frac{CH_4}{V \times t} \quad (1)$$

where CH_4 is the methane concentration, $^{14}CO_2$ is the activity of the produced carbon dioxide, $^{14}CH_4$ is the activity of the radioactive methane, t is the incubation time and V is the volume of the samples. The method itself does not distinguish between MOx and AOM but it can be assumed that MOx occurs only in the top oxygenated sediment horizons, based on previous in situ microsensor measurements (de Beer et al. 2006).

SR rates were calculated with the following equation:

$$SR = \frac{TRI^{35}S}{(^{35}SO_4^{2-} + TRI^{35}S)} \times \frac{SO_4^{2-}}{V \times t} \quad (2)$$

where SO_4^{2-} is the sulfate concentration, $TRI^{35}S$ is the activity of the reduced sulfur compounds and $^{35}SO_4^{2-}$ is the radioactive sulfate (Treude et al. 2003).

Total benthic oxygen uptake—The TOU and the methane emission rates were determined with a cylindrical benthic chamber module (Fig. 2B). These measurements were conducted in 2007 (ARK XXII-1b) and 2009 (ARK XXIV-2). The benthic chamber was operated by the ROV, and the water height inside the chamber was determined by visual observation with the ROV camera system. The stirred chamber (radius 9.5 cm) enclosed a seafloor area of

Table 1. Overview of all measurements and PC sampling stations (MOx = methane oxidation; SR = sulfate reduction) investigated in this study. The data are available online at http://doi.pangaea.de/10.1594/PANGAEA.744547.

Year	Cruise	Habitat	Measurements	PANGAEA database event labels
2001	HMMV	warm center	MOx	AWI_ATL_D5/PUC-1
		Beggiatoa mat	MOx	AWI_ATL_D4/PUC-1; AWI_ATL_D5/PUC-2; AWI_ATL_D5/PUC-3;
		siboglinid tubeworms	MOx	AWI_ATL18; AWI_ATL22
2003	ARK XIX-3b	hot center	SR	PS64/312-1; PS64/314-1
			MOx	PS64/312-1; PS64/314-1
		warm center	SR	PS64/377_PUC-1; PS64/377_PUC-2; PS64/372-1; PS64/332-1; PS64/373-1
			MOx	PS64/377_PUC-1; PS64/377_PUC-2; PS64/372-1
		gray mat	SR	PS64/347_PUC-1; PS64/347_PUC-2; PS64/347_PUC-3;PS64/377_PUC-14; PS64/377_PUC-23; PS64/377_PUC-27
			MOx	PS64/347_PUC-1; PS64/347_PUC-2; PS64/347_PUC-3; PS64/377_PUC-14; PS64/377_PUC-23; PS64/377_PUC-27; VKGD277/PC-10;
		Beggiatoa mat	SR	PS64/317_PUC-17; PS64/317_PUC-8; PS64/322-1; PS64/371-1
			MOx	PS64/317_PUC-17; PS64/317_PUC-14; PS64/322-1
		siboglinid tubeworms	SR	PS64/326_PUC-7; PS64/326_PUC-8; PS64/326_PUC-12; PS64/341-1; PS64/374-1; PS64/336-1
			MOx	PS64/326_PUC-7; PS64/326_PUC-8; PS64/326_PUC-12; PS64/341-1; PS64/374-1; PS64/336-1
2006	Viking	gray mat	SR	VKGD277/PC-1, VKGD277/PC-3
			MOx	VKGD277/PC-10; VKGD277/PC-11
		Beggiatoa mat	SR	VKGD276/PC-13; VKGD276/PC-2; VKG MTP 6;
			MOx	VKGD276/PC-1; VKGD276/PC-3
2007	ARK XXI-1b	warm center	benthic chamber	PS70/119-1_CALMAR-1; PS70/125-1_CALMAR-1
		gray mat	benthic chamber	PS70/112-1_CALMAR-1; PS70/125-1_CALMAR-2
			SR	PS70/064-1_PUC-26; PS70/052-1_PUC-16
		next to gray mats	benthic chamber	PS70/112-1_CALMAR-2
		Beggiatoa mat	benthic chamber	PS70/052-1_CALMAR-1;PS70/130-1_CALMAR-1
			SR	PS70/096-1_PUC-18; PS70/096-1_PUC-23; PS70/112-1_PUC-23; PS70/112-1_PUC-13; PS70/112-1_PUC-34; PS70/112-1_PUC-11
		next to *Beggiatoa* mat	benthic chamber	PS70/130-1_CALMAR-1
		siboglinid tubeworms	benthic chamber	PS70/105-1_CALMAR-1
2009	ARK XXIV-2	hot center	benthic chamber	PS74/0183-1_CALMAR-1; PS74/0188-1_CALMAR-1
			SR	PS74/169-1_PUC-3; PS74/169-1_PUC-8; PS74/169-1_PUC-9
			MOx	PS74/169-1_PUC-3; PS74/169-1_PUC-8; PS74/169-1_PUC-9
		warm center	SR	PS74/168-1
			MOx	PS74/168-1
		Beggiatoa mat	SR	PS74/172-1_PUC-116; PS74/172-1_PUC-131; PS74/172-1_PUC-140
			MOx	PS74/172-1_PUC-116; PS74/172-1_PUC-131; PS74/172-1_PUC-140
		siboglinid tubeworms	SR	PS74/136-1
			MOx	PS74/136-1

284 cm^2 together with 10–15 cm (equivalent to 4–6 liters) of overlying bottom water. A valve in the chamber lid ensured the release of overpressure while placing the chamber gently into the sediment avoiding any disturbance of the sediment surface. Two Clark-type oxygen mini-electrodes mounted in the chamber lid continuously monitored the oxygen concentration in the enclosed water. A two-point calibration of the reading of the mini-electrodes was performed. The reading at zero O_2 concentration was taken on board at in situ temperature. Values for the bottom water O_2 concentration were determined in situ at the seafloor. The respective oxygen concentration of the bottom water was determined by Winkler titration of water samples or from in situ readings with an oxygen optode (a component of the Recording Current Meter 11 (Aanderaa). In addition to the sensor readings, five water samples were taken with 50-mL syringes at preprogrammed time intervals to determine the dissolved methane concentration. After retrieval of the chamber, the water samples were immediately preserved by adding 40 mL to sealed glass vials with NaOH pellets. The samples were stored at 4°C until further analyses in the home laboratory. Methane concentrations were measured by gas chromatography (5890A; Hewlett Packard).

The TOU and methane emission rates were calculated from the linear regressions of concentration vs. time

(mmol m^{-2} d^{-1}):

$$\text{TOU/methane emission} = \frac{dC}{dt} \times \frac{V_{chamber}}{A_{chamber}} \quad (3)$$

where dC/dt (μmol L^{-1} h^{-1}) are the changes of concentrations over the incubation time, $V_{chamber}$ (cm^3) is the volume of the overlying water in the enclosed chamber, and $A_{chamber}$ (cm^2) is the area of the sediment enclosed by the chamber. Calculating the potential replacement of oxygen-rich bottom water with oxygen-free subsurface water during the incubation of the chamber indicates that $< 1\%$ of the enclosed water volume could have been replaced by subsurface fluids during the 4–6-h incubation time.

In situ sediment temperature measurements—In situ temperature measurements at shallow sediment depths using ROV-operated temperature probes were conducted in 2003, 2005, 2006 (Feseker et al. 2008), and in 2007 (Pérez-Garcia et al. 2009). The mechanical design of the probes and the number of temperature sensors varied between the different cruises, but all temperature measurements covered the interval from around 0–50 cm below the seabed. The sensors were calibrated to a precision of 0.002°C (Feseker et al. 2008; Pérez-Garcia et al. 2009).

Areal budget calculations—For a budget of total oxygen and methane fluxes at the entire HMMV geostructure and within the different habitats, measurements from five cruises were compiled (Fig. 1). Previous estimates of methane budgets for mud volcano systems (Linke et al. 2005; Sauter et al. 2006; Sommer et al. 2009) have relied on a small number of measurements at selected locations. Here we integrated rate measurements over 9 yr at HMMV, assuming that the different assemblages of benthic organisms are associated with persistent biogeochemical and geophysical settings (Fig. 1), as described previously (de Beer et al. 2006; Niemann et al. 2006; Lichtschlag et al. 2010). Videographic observations during ROV sampling indicated minor changes in overall habitat distribution within this time period. Hence, we have based the areal calculations on the detailed habitat map obtained in 2003 (Jerosch et al. 2007). The gray mat habitat (III) was only recently described (de Beer et al. 2006; Lichtschlag et al. 2010) and not considered as separate habitat in the previous habitat analyses (Jerosch et al. 2007). Based on the published data and our video observations, we assumed that on average 75% of the hummocky area was inhabited by siboglinid tubeworms. The remaining 25% of this area was devoid of tubeworms but hosted patchily distributed gray mats (III).

To account for the heterogeneous distribution of organisms for areal budget calculations, we distinguished between those zones marked by 100% coverage of the seafloor by chemosynthetic organisms and zones with a patchy coverage. The benthic chamber measurements for oxygen uptake and methane emission rates were performed in the different zones of each habitat (i.e., on seafloor with 100% coverage with bacterial mats, and next to the mats in zones with more patchy distributions). Subsequently, we used both measurements in the respective proportion to calculate the total areal fluxes. Areal estimates of sulfate and methane turnover were gained by depth integration of sulfate reduction and methane oxidation rates in the respective habitats for the upper meter of seabed. This depth was chosen to account for the high subsurface AOM and SR rates below the roots of the siboglinid tubeworms (Lösekann et al. 2008).

Results

In situ temperature measurements—Ninety-four in situ sediment temperature measurements (Fig. 2E) were carried out in specific habitats based on visual observations recorded as digital photographs during the ROV dives. The locations of all measurements are shown in Fig. 3. All temperature measurements on the HMMV seafloor showed elevated gradients compared to the regional background geothermal gradient (0.07°C m^{-1}; Table 2). In the HMMV central area (I), the highest temperature gradients were reached in an area characterized by a disturbed seafloor surface (Table 2; Fig. 2A), < 100 m in diameter, and north of the geometrical center of the mud volcano. In this 'hot center' area, the temperature gradients ranged between 10°C m^{-1} and 46°C m^{-1} with a mean of 25.9°C m^{-1}. Around the hot center, smoother mud deposits form a large flat area extending up to 150 m south and east of the hot center. These smooth mud deposits were associated with much lower temperature gradients between 1.5°C m^{-1} and 17°C m^{-1} (Table 2) and are subsequently called warm center area (Fig. 2B).

Measurements in the white (II) and gray mat (III) habitats showed lower average temperature gradients than in the hot and warm center, but were not significantly different from each other (Table 2). In the *Beggiatoa* mat habitat (II) the temperature gradients varied between 1.2°C m^{-1} and 20.8°C m^{-1} inside the white mats and between 0.9°C m^{-1} and 11.3°C m^{-1} next to the white mats. The difference between the average temperature gradients inside and next to white mats was, however, not significant. In the transition zone where gray mats (III) occurred, the temperature gradients ranged from 0.6°C m^{-1} to 6.7°C m^{-1} next to gray mats and from 2°C m^{-1} to 6°C m^{-1} inside gray mats. Again, the difference between the average temperature gradients inside and next to gray mats was not significant. In the siboglinid tubeworm habitat north of the center (IV) in total six in situ temperature measurements were conducted. Here, the lowest mean temperature gradient (2.0°C m^{-1}) was found. The difference with next-to-the-tubeworm patches (5.9°C) and several other HMMV habitats were, however, not statistically significant (Table 2).

Methane and sulfate turnover in different HMMV habitats—Center (I): In the center, methane oxidation and sulfate reduction rates were measured in 2001, 2003, and 2009, and were similar in all years (Fig. 4A,B). Furthermore, methane and sulfate turnover were not significantly different in the warm and hot center. At the sediment surface where oxygen is available (de Beer et al. 2006) methane oxidation rates of up to 385 nmol cm^{-3} d^{-1} (hot center) were observed. SR was low (< 20 nmol cm^{-3}

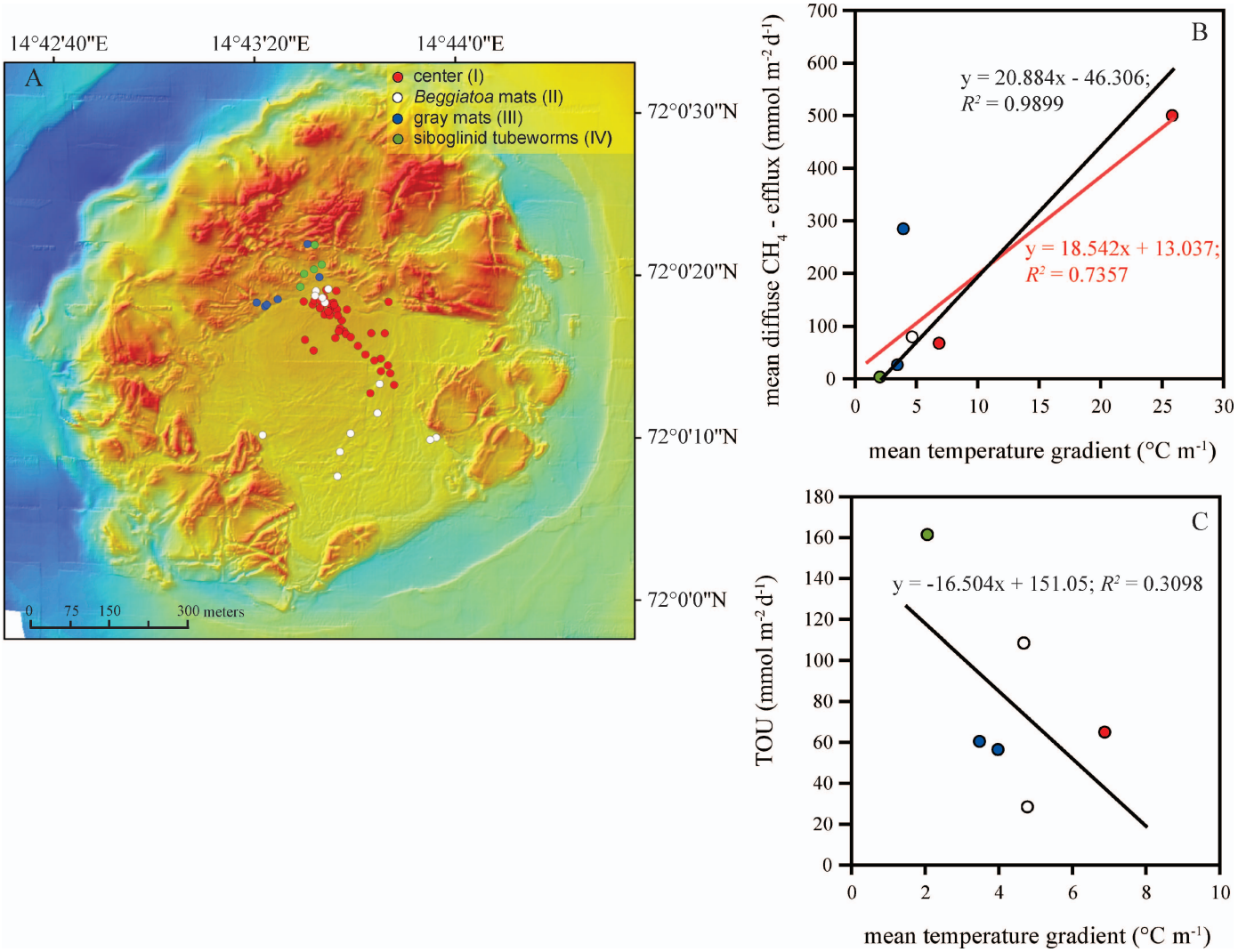

Fig. 3. (A) Positions of the shallow seafloor temperature measurements; (B) mean methane flux vs. mean temperature gradients and corresponding regression lines with (red line) and without data next to gray mats (black line, for details see text); (C) TOU vs. mean temperature gradient including fit and regression line. The data points are color coded for the different habitats in accordance with (A). Please note the different scales of the temperature gradients in (B) and (C).

d^{-1}) in all replicates over the entire vertical profile down to 19 cm below seafloor (bsf) and was $<$ 1 nmol cm^{-3} d^{-1} below 20 cm. Hence, the center was dominated by aerobic methane oxidation, as previously described (Niemann et al. 2006). On average, the integrated rates of methane oxidation over 1 m of seafloor in the hot and warm center were 5.0 (n = 7; ± 5.0 SD) and 3 (n = 4; ± 4.6 SD) mmol m^{-2} d^{-1}, respectively (Table 3). For SR the depth-integrated rates were only 0.8 (n = 7; ± 0.2 SD) and 1.0 mmol m^{-2} d^{-1} (n = 8; ± 0.4 SD) for the hot and warm center area, respectively.

Beggiatoa mat (II): Below the *Beggiatoa* mats, the highest methane consumption rates of up to 418 nmol cm^{-3} d^{-1} were found in the anoxic 1–2 cm sediment layer, decreasing with increasing depth (Fig. 4C,D). The sulfate reduction rates followed the same trend with a peak of up to 1353 nmol cm^{-3} d^{-1} in 1–3-cm depth, reaching $<$ 20 nmol cm^{-3} d^{-1} below 15 cm. The depth-integrated mean values for AOM and SR were 9.8 (± 6.6 SD; n = 20) and 14.2 (± 6.2 SD; n = 35) mmol m^{-2} d^{-1}, respectively (Table 3). It has to be noted that both methane and sulfate turnover rates varied up to two orders of magnitude between different habitats within the same year, and in the case of the *Beggiatoa* mats and the siboglinid tubeworms also within the habitat between different years. Covering the spatial variability within a habitat at HMMV seems to be more important for accurate areal turnover-rate estimates than variations between different years. The spatial variability most likely results from small-scale heterogeneities in methane conduits through the seafloor, but may also be related to variations in the microbial community composition (Lösekann et al. 2008). However, we cannot exclude that short-term (hours to days) temporal changes in fluid and methane flow also influence local rate measurements.

Table 2. Shallow sediment temperature gradients of the different HMMV habitats (n = number of replicates; recorded in the upper 50 cm of seafloor). Mean and median (not shown) of the temperature measurements were not significantly different.

Habitat	°C m^{-1}			
	Minimal	Maximal	Mean	CI(95%)
(I) Center				
Hot(n=16)	10.3	46.0	25.9	21.3–30.6
Warm(n=37)	1.5	17.2	6.9	5.7–8.0
(II) *Beggiatoa* mat				
Beggiatoa mat(n=11)	1.2	20.8	4.7	1.2–8.3
'Next to'(n=9)	0.9	11.3	4.8	2.4–7.1
(III) Gray mat				
Gray mat(n=8)	0.6	6.7	4.0	3.0–4.9
'Next to'(n=7)	2.0	6.0	3.5	2.0–5.0
(IV) Siboglinid tubeworms				
Tubeworms(n=4)	0.9	3.7	2.0	0.9–3.3
'Next to'(n=2)	3.4	8.3	5.9	1.1–10.7

Gray mat (III): In 2003 and 2006, methane oxidation and sulfate reduction rates were measured in the transition zone between the warm center and the tubeworm-covered hills of the HMMV, characterized by the occurrence of patchy gray mats (Fig. 2D,E). Additionally, SR rates were also determined in 2007 at gray mat patches. The highest consumption rates of sulfate and methane were found distributed over the uppermost 10 cm of the sediment (Fig. 4E,F). Minimal and maximal AOM and SR rates were covering a wide range of 10–402 nmol cm^{-3} and 8–1918 nmol cm^{-3} d^{-1}, respectively. The average depth-integrated AOM and SR rates were 10.7 (± 9.4 SD; n = 7) and 43.3 (± 34.5 SD; n = 11) mmol m^{-2} d^{-1} (Table 3).

Siboglinid tubeworms (IV): Consumption of methane and sulfate in sediments inhabited by siboglinid tubeworms were determined in 2001, 2003, and 2009 (Fig. 4G,H). Down to 45 cm bsf, methane oxidation (n = 17) and sulfate reduction (n = 15) rates were low. Below this depth, around the roots of the tubeworms, AOM and SR rates increased markedly with maximal SR rate of nearly 1700 nmol cm^{-3} d^{-1} at 45-cm depth. On average the integrated AOM and SR rates were 20.7 (± 5.4 SD; n = 17) and 56.3 (± 79.5 SD; n = 15) mmol m^{-2} d^{-1} (Table 3).

Fluxes of oxygen and methane at the HMMV—Benthic chamber measurements were performed in all main HMMV habitats in 2007, and additionally in the hot center in 2009 (Table 1). Because of the limited dive time, the number of benthic chamber incubations was lower compared to other measurements, limiting the statistical analysis of relationships of oxygen and methane fluxes with other parameters. However, at least two in situ flux measurements were performed per habitat, which is the most comprehensive data set currently available for any seep ecosystem. The highest temperature gradients (Table 2) correlated with the highest methane efflux (498 mmol m^{-2}d^{-1}) at the hot center, the lowest with the siboglinid tubeworm area (Table 3). Average temperature gradients and methane efflux to the hydrosphere decreased with increasing distance from the hot center, in the order of hot center > warm center > gray mats > *Beggiatoa* mats > siboglinid tubeworms. The diffuse CH_4 flux was correlated with the average temperature gradient (R^2 = 0.74), except in the transition zone north of the hot center toward the siboglinid tubeworm zone, where the second highest methane efflux was found next to the gray mats (Fig. 3). This transition zone was characterized by small patches of gray mats and was highly heterogenic in space and time; hence, not enough replicate measurements could be obtained. When excluding this data point, the correlation reached an R^2 = 0.99. Both the microbiological oxidation of methane (R^2 = 0.3) and reduction of sulfate (R^2 = 0.4) were negatively correlated with the temperature gradient (Table 3). In contrast, no simple linear correlation was detected between the temperature gradient and TOU, although the lowest TOU was found in the hot center sediment, and the highest was associated with the siboglinid tubeworms (Fig. 3). Furthermore, the in situ oxygen uptake exceeded by far the sulfide flux estimated from ex situ measured AOM and SR rates, indicating that in situ sulfide production could be much higher, or that aerobic methane and sulfide oxidation at the sediment surface contribute substantially to the total oxygen consumption.

Comparing the TOU of sediment areas populated by microbial mats to their direct surrounding on a scale of decimeter to meter, a substantial difference was detected. TOU of sediment densely covered by *Beggiatoa* mats (108 mmol m^{-2} d^{-1}) was more than three times higher than that of the bare sediment next to the mat. Between the two mat communities, *Beggiatoa* mats showed higher oxygen uptake and methane emission rates than gray mats, but methane consumption was similar in both habitats.

Discussion

The spatial gradient in fluid flow rates across the HMMV has been found to create different niches for benthic assemblages, characterized by specific transport regimes and biogeochemical settings (de Beer et al. 2006; Jerosch et al. 2007; Feseker et al. 2008). Some temporal variability of mud volcanism was indicated by changes in absolute seafloor temperature between the different years (Feseker et al. 2008), and variations in the microbathymetry of mud flows in the central and southern HMMV (Foucher et al. 2009). However, the main biogeochemical habitats appear to be rather stable in their spatial distribution and function, supporting chemosynthetic communities and associated benthic fauna (Van Gaever et al. 2006, 2009*a*).

By targeted in situ quantification of oxygen, methane, and sulfide fluxes during several expeditions to the HMMV we developed a spatial budget for the different HMMV habitats, including a first estimate of internal patterns (< 10 m scale). It is known that the fragmented habitat structure of cold seep systems and the dynamics of methane fluxes cause a high spatial heterogeneity within the targeted habitats (Sibuet and Olu 1998). Using spatially replicate

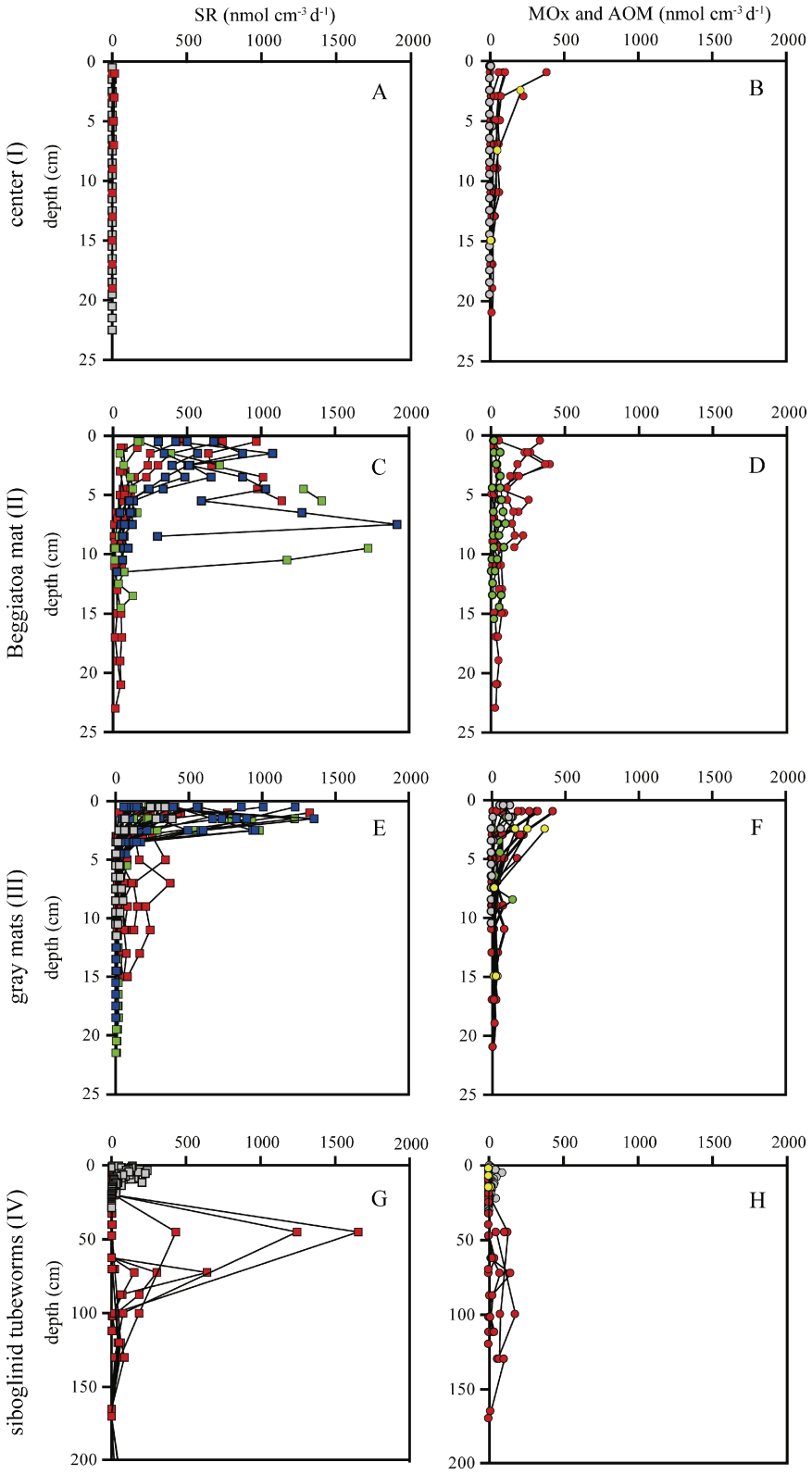

Fig. 4. Left panel: Rates of sulfate reduction and right panel: methane oxidation in different habitats. (A–B) center (I; hot and warm center show similar rates); (C–D) *Beggiatoa* mat (II); (E–F) gray mat (III); (G–H) siboglinid tubeworm (IV) habitat. The symbols of the different years are color-coded: yellow = 2001, red = 2003, green = 2006, blue = 2007, and gray = 2009. (G–H) note the different depth scales. (A–F) only PC measurements are shown, the GC measurements had rates < 10 nmol cm^{-3} d^{-1} down to 1-m sediment depth.

Table 3. Average temperature gradients and fluxes in different habitats of the HMMV. All numbers are given in mmol m^{-2} d^{-1} if not indicated otherwise. The sulfate reduction (SR) and methane oxidation rates (MOx and AOM) were integrated over the top meter of sediment. Total oxygen uptake (TOU) and methane emission (CH_4 efflux) rates were measured with the benthic chamber. The methane efflux refers only to diffuse transport of methane from the seafloor to the hydrosphere. Both values are given when only two measurements were performed. Total methane flux is calculated as the sum of CH_4 efflux and oxidation; the efficiency of the biological methane sink is calculated as the percent consumption of methane from the total methane flux. n = number of replicates; nd = not determined.

	Center (I)		*Beggiatoa* mat (II)		Gray mat (III)		Siboglinid tubeworms (IV)	
(mmol m^{-2} d^{-1})	Hot	Warm	*Beggiatoa*	'Next to'	Gray mat	'Next to'	Tubeworm	'Next to'
Temperature gradients	25.9°C m^{-1}	6.9°C m^{-1}	4.7°C m^{-1}	4.8°C m^{-1}	4.0°C m^{-1}	3.5°C m^{-1}	2.0°C m^{-1}	5.9°C m^{-1}
Total CH_4 flux	>500	61–78	88	nd	36	>280(rates nd)	23	nd
CH_4 efflux	220; 777(n=2)	58; 75(n=2)	78(n=1)	nd	25(n=1)	251; 315(n=2)	2(n=1)	nd
Sedimentary MOx and AOM	5.0±5.0(n=7)	3±4.6(n=4)	9.8±6.6(n=20)	nd	10.7±9.4(n=7)	nd	20.7±5.4(n=17)	nd
Sedimentary SR	0.8±0.2(n=7)	1.0±0.4(n=8)	14.2±6.2(n=35)	nd	43.3±34.5(n=11)	nd	56.3±79.5(n=15)	nd
Biological methane sink (% of total flux)	<3	4	11	nd	30	nd	90	nd
TOU	15; 66(n=2)	57; 72(n=2)	101; 114(n=2)	28(n=1)	60(n=1)	33; 78(n=2)	161(n=1)	nd

measurements, we investigated: (1) the link between seafloor temperature gradients, methane efflux, and oxygen consumption, (2) the internal relation between oxygen, methane, and sulfide fluxes, and (3) the efficiency of the biological filter against methane emission to the hydrosphere.

Relation between temperature gradients, methane flux, and oxygen consumption at HMMV—In situ temperature measurements from three cruises in 2003, 2005, and 2006 suggest that the sediment temperature distribution at the HMMV is controlled largely by fluid flow (Feseker et al. 2008). Warm subsurface pore waters rising through a deep conduit transport high amounts of methane to the seafloor. Rates of vertical specific discharge were estimated to increase from < 1 m yr^{-1} at the border of the central area to > 5 m yr^{-1} in the warm center associated with temperature gradients above 4°C m^{-1} (Feseker et al. 2008). For the disturbed seafloor area with the highest temperature gradient, fluid flow has not been estimated yet. The temperature measurements reported in this paper attest to the high activity of the HMMV. In addition, we have obtained the first in situ measurements of methane efflux for the main habitats of the HMMV, which show a strong relation with the temperature gradients (Table 3) and, hence, most likely also to fluid flow. Previously, it was debated whether the spatial and temporal variation of temperature gradients at the HMMV are caused by fluid flow dynamics or local patterns in mud eruptions (Feseker et al. 2008). The spatial correlation between dissolved methane efflux and temperature gradients supports the hypothesis that fluid flow is important for temperature gradient variations in space and time.

Local rates of dissolved methane efflux at the HMMV of up to 777 mmol m^{-2} d^{-1} in the hot center (Table 3) are the highest emission rates so far published for cold seep ecosystems (< 265 mmol m^{-2} d^{-1}, polychaete assemblage, Hikurangi Margin [New Zealand; Sommer et al. in press]; 1.9–100 mmol m^{-2} d^{-1}, *Beggiatoa* mats, Hydrate Ridge [Torres et al. 2002; Sommer et al. 2006]; < 1 mmol m^{-2} d^{-1}, tubeworm habitat, Captain Artyunov mud volcano [Sommer et al. 2009]). However, the methane efflux rapidly decreased together with the temperature gradient from the hot center to the border of the warm center, within a distance of $\sim$ 200 m. At the rim of the center, *Beggiatoa* mats and the gray mats of the transition zone showed similar temperature gradients and methane effluxes of around 25–78 mmol m^{-2} d^{-1}, resembling the high fluxes measured in *Beggiatoa* mats at Hydrate Ridge (Sommer et al. 2006). With 2 mmol m^{-2} d^{-1}, methane efflux was much lower in the outer hummocky area populated with tubeworms. In this zone, tubeworm-free patches were associated partly with gray mats and higher mean temperature gradients > 4°C m^{-1} (Table 3) compared to the tubeworm patches. Although these differences were not statistically significant, the data indicate that locally enhanced flow of anoxic fluids could limit the growth of tubeworms. This was also suggested by visual observations with the ROV, showing the exclusion of tubeworms from high fluid flow areas such as Beggiatoa mats or the central mud flows.

Using averaged diffuse methane effluxes for areal integrations, the entire HMMV had an estimated emission of dissolved methane to the hydrosphere of 37×10^3 mol d^{-1}, or 14×10^6 mol yr^{-1}. Previously, total gas bubble emission has been recorded in 2003 with a rate of 8–35 $\times$ 10^6 mol CH_4 yr^{-1}, based on measurements at three active vents of the HMMV (Sauter et al. 2006). The release of gas bubbles can vary by orders of magnitude spatially and temporally, depending on patterns in hydrate content, fluid flow and leakage pathways. The finding that diffuse methane efflux from mud volcanoes may be as high as focused, gaseous efflux, is very important for future exploration and biogeochemical studies of cold seep ecosystems.

In this study, we also investigated the relationship between methane efflux and total oxygen consumption. Where methane flux limits the activity, growth, and sustainability of cold seep communities, one could expect a strong relationship with total oxygen consumption. However, for the HMMV it was previously proposed that due to the very high fluid flow rates of $>$ 1m yr^{-1}, the availability of electron acceptors to benthic communities might be exerting the strongest control of their distribution and activity (Niemann et al. 2006). Accordingly, methane flux and oxygen consumption show a negative relationship across the HMMV ecosystem, with lowest consumption rates in the hot center characterized by the highest temperature gradients and fluid flow rates, and the highest consumption rates in the *Beggiatoa* mats and tubeworm fields, associated with low fluid flow rates.

Dissolved and total oxygen uptake vs. methane and sulfate consumption—Oxygen is the terminal electron acceptor of aerobic and anaerobic processes in marine sediments (Glud 2008). For methane seeps, one could assume that oxygen consumption can be used to quantify the total biological sink for methane because oxygen is used either directly for the aerobic methane oxidation or indirectly for re-oxidation of reduced compounds like sulfide, a product of the AOM process. The recycling of chemosynthetic biomass production derived from sulfide or methane oxidation could also be a sink for oxygen (Lichtschlag et al. 2010).

Previously, total oxygen consumption at cold seep ecosystems was found to be very high, exceeding TOU of nonseep benthic communities by one to two orders of magnitude. For example, at Hydrate Ridge, TOU rates of 38 and 53 mmol m^{-2} d^{-1}; (Sommer et al. 2006) were found, and even higher TOU were reported from seeps of the Peru (105 mmol m^{-2} d^{-1}) and Cascadia margin (1600 $\pm$ 300 mmol m^{-2} d^{-1} [Linke et al. 1994; Suess et al. 1999]). At the HMMV, TOU varied between the different habitats by one order of magnitude from 15 mmol m^{-2} d^{-1} to 161 mmol m^{-2} d^{-1}. Even the lowest rates measured in the center were five-fold higher than in sediments from the pelagic Norwegian margin (3.1 mmol m^{-2} d^{-1}; Sauter et al. 2001). The TOU gained from benthic chamber incubations covers not only total microbial and faunal oxygen respiration in the sediments, but also fauna-mediated chemical consumption enhanced by bio-turbation and bio-irrigation and small-scale sediment topography (Røy et al. 2002; Wenzhöfer and Glud 2002; Glud et al. 2003).

Studies of coastal and continental slope sediment demonstrated that TOU could be up to four-fold higher than diffusive oxygen uptake (DOU). Differences in the oxygen consumption rates obtained by the two methods were found to correlate with abundances of in- and epifauna in these habitats (Wenzhöfer and Glud 2002; Glud 2008). Only little is known about the relationship between dissolved and total oxygen consumption with methane and sulfate consumption at cold seeps. Cold seeps support high benthic biomass and activities, which were found to be related to total methane efflux, and most likely sulfide production from AOM (Sibuet and Olu 1998). Here we tested whether we could find relationships between dissolved and total oxygen consumption, and with methane and sulfate consumption as the main energy-yielding processes at the HMMV. In theory, the stoichiometric relationship between TOU and AOM or SR should be 1 : 2. Under the assumption that the system is in balance, methane is the sole electron donor, all methane is oxidized anaerobically by sulfate reduction to sulfide, and all sulfide is respired with oxygen. Deviations could result from an efflux of methane into the aerobic zone, fueling aerobic methanotrophy with a stoichiometry of oxygen-to-methane consumption between 1 : 1 and 1 : 2 (depending on growth efficiency; Naguib 1976), and on variations in the trophic food web. However, the spatial variation in efflux of methane, benthic community composition and biomass, and methane consumption rates suggested no stoichiometric link between TOU and AOM at the HMMV.

The main problem with a direct comparison is the difference between in situ assessment of TOU and the ex situ quantification of methane and sulfate consumption, the latter likely suffering artifacts from the difference in sulfate and methane availability after retrieval of the cores. Depending on the fluid flow within the seafloor, this may result in either an overestimation (high fluid flow rates - sulfate dependency) or underestimation (low fluid flow rates - methane dependency) of the turnover rates. The pore waters of retrieved cores are enriched in sulfate by gas ebullition and a reflux of the overlying seawater, potentially causing higher SR rates. In contrast, the retrieval reduces methane availability due to depressurization. In the following, the difference in the relationship between TOU and sulfide production from methane oxidation is discussed in detail for each habitat.

Center (I): Sulfide production provided only a very small amount of reducing power for TOU, indicating that AOM was largely absent due to the high upward flow rates of sulfate-free subsurface fluids (de Beer et al. 2006). Still, TOU at the HMMV center was an order of magnitude higher than at sediments from the pelagic Norwegian margin, suggesting that methane was the main electron donor for oxygen consumption (ratio of 1 : 2). However, the in situ TOU (57–72 mmol m^{-2} d^{-1}) measured was $>$ 20 times higher than the ex situ methane oxidation rates and five-fold higher compared to previous DOU measurements (de Beer et al. 2006; Lichtschlag et al. 2010). Interestingly,

highest methane efflux in the hot center correlated with higher heat gradients and lower TOU compared to the warm center.

Previously, Lösekann et al. (2007) as well as Elvert and Niemann (2008) found abundant aerobic methane-oxidizing bacteria in surface sediments of the center. Also, the observed differences between TOU and DOU could not be explained by the presence of benthic fauna, which had only very low abundances (Van Gaever et al. 2006). Hence, we suggest that the assemblage of aerobic methane-oxidizing bacteria associated with surface sediments of the mud volcano center (Lösekann et al. 2008) may cause considerable oxygen consumption that was not detected with microsensors.

Beggiatoa mat (II): Below the *Beggiatoa* mats, the integrated consumption rates of sulfate and methane in the mud volcano sediments appear stable over time (Niemann et al. 2006), both temporally as well as spatially. The measurements indicate an active AOM-SR zone close to the sediment surface mainly in the first 3 cm of the sediment with a relatively close coupling of sulfate and methane turnover. However, also in the *Beggiatoa* mat habitat, considerable differences between DOU and TOU, as well as TOU and sulfide production, were found.

Previously measured DOU (22 mmol m^{-2} d^{-1} [de Beer et al. 2006; Lichtschlag et al. 2010]) were only 20% of TOU (Table 3) suggesting that benthic fauna could play a major role in the oxygen consumption, or that considerable reoxidation of methane and sulfide occurs above the seafloor, not detected by microsensor measurements. Investigations of the faunal community structure showed that the meiobenthos consists nearly exclusively of the nematode species *Halomonhystera desjuncta* (Van Gaever et al. 2006, 2009*a*). This small invertebrate ($\sim$ 1 mm) is not associated with any microbial ecto- or endosymbionts. Isotopic data suggest that these nematodes are heterotrophic, feeding on the biomass of the sulfide oxidizing bacteria (Van Gaever et al. 2006, 2009*a*). The nematode is highly abundant (11×10^6 individuals m^{-2}) in the HMMV *Beggiatoa* mat habitats (Van Gaever et al. 2006). Considering an average deep-sea nematode respiration rate of 2.7 nmol O_2 d^{-1} $individual^{-1}$ (Shirayama 1992), the entire nematode community could consume $\sim$ 30 mmol O_2 m^{-1} d^{-1}. These nematodes were far less abundant in the gray mat habitat (III), which also showed a lower TOU despite the higher sulfide fluxes. Hence, we conclude that a substantial fraction of TOU in the *Beggiatoa* mats is explained by the activity of the faunal community, rather than by direct sulfide oxidation.

The TOU of the *Beggiatoa* mat was three times higher than the total sulfide production estimated from SR, indicating that aerobic oxidation of methane in the mat also played a significant role, as in the center habitat. Previously, aerobic methane-oxidizing bacteria were found associated with the *Beggiatoa* mat (Elvert and Niemann 2008), supporting this hypothesis. The methane flux (78 mmol m^{-2} d^{-1}) across the sediment surface would be sufficient to fuel a considerable proportion of oxygen consumption in the top few micrometers of the bacterial mat (de Beer et al. 2006; Lichtschlag et al. 2010).

Gray mat (III): Patches of gray mats consisting of diverse bacteria involved in sulfur cycling occur in the transition zone between the hot center (I) and the siboglinid tubeworm zone (IV), as well as within the siboglinid tubeworm area (IV; Fig. 1B). Some of the gray mats appear overgrown by *Beggiatoa* indicating that they could be pioneer communities, replaced by *Beggiatoa* mats when fluid flow conditions stabilize. Accordingly, the meiobenthos of the HMMV gray mats (IV) consists mostly of the nematode species *H. desjuncta*, but in much lower numbers than in the *Beggiatoa* mats. Applying the mean deep-sea nematode respiration rate of 2.7 nmol O_2 d^{-1} $individual^{-1}$ (Shirayama 1992) to their abundance (1.1×10^6 individual m^{-2}) within the gray mats (Van Gaever et al. 2009*b*), the oxygen consumption of the meiobenthos could be in the range of 3 mmol m^{-2} d^{-1}, hence explaining only a small proportion of the total consumption. Accordingly, the gray mat TOU (average in and next to gray mats: 57 mmol m^{-2} d^{-1}) was not much higher than the DOU rates (de Beer et al. 2006; Lichtschlag et al. 2010) and could be entirely consumed in the reoxidation of the sulfide flux (43 mmol m^{-2} d^{-1}) from the underlying sediments (Fig. 4E,F).

Siboglinid tubeworms (IV): By far the largest area of the HMMV is inhabited by siboglinid tubeworms (IV; Fig. 1D), extending their roots deep into the sediments to take up hydrogen sulfide from the AOM zone above methane hydrates (de Beer et al. 2006; Niemann et al. 2006; Lösekann et al. 2008). The sulfide is oxidized by their thiotrophic endosymbionts (Naganuma et al. 1999, 2005; Lösekann et al. 2008), releasing sulfate back into the seafloor. Investigations on siboglinid tubeworms from the Gulf of Mexico showed their potential to excrete 70–90% of the recycled sulfate again to the surrounding sediment and, therefore, enhance further the sulfide production (Dattagupta et al. 2006, 2008). Accordingly, we found the highest areal AOM and SR rates as well as TOU in the tubeworm habitat (Table 3).

The main energy source for the worm's endosymbionts is sulfide and it can be assumed that the oxygen (161 mmol m^{-2} d^{-1}) consumed in this habitat is mainly used for sulfide oxidation. This would require SR and AOM rates of $\sim$ 80 mmol m^{-2} d^{-1}, which is higher than the range of the measured ex situ methane and sulfate turnover rate (Table 3). Investigations in tubeworm-inhabited sites at the Captain Arutyunov mud volcano (Gulf of Cadiz) indicate that aerobic methane oxidation by free-living methanotrophic bacteria is a relevant process due to bio-irrigation of the sediments by tubeworms (Sommer et al. 2009).

The efficiency of the biological filter: Methane efflux vs. methane consumption—Comparing methane fluxes across all habitats (Tables 3, 4), it can be concluded that the center (I) is the main site of diffuse efflux of methane at the HMMV. This is coherent with high bottom-water methane concentrations of $> 10^4$ nmol L^{-1}, which were reported before from the central HMMV area (Sauter et al. 2006). Previously, the efficiency of the microbial filter against methane at HMMV was estimated by comparing methane

Table 4. Total oxygen consumption (TOU) rates, total diffuse methane emissions, and consumption rates of methane and sulfate for all HMMV habitats, and the entire ecosystem. The calculations are based on the fluxes in Table 3. All values are in ($\times 10^3$) mol d^{-1}. Estimates of sizes of HMMV habitats were modified from Jerosch et al. (2007). Areal methane consumption is calculated as the percent of methane consumption (MOx + AOM) from the total methane flux. Gaseous methane escape was previously estimated with 22–96 ($\times 10^3$) mol d^{-1}.

Habitat	Area ($\times 10^3$) m^2	Total methane flux	CH_4 efflux	MOx+AOM	SR*	TOU	Areal CH_4 consumption efficiency (% of total flux)
		($\times 10^3$) mol d^{-1}					
(I) Center							
Hot center	14	7.1	7.0	0.1	<0.1	0.6	1
Warm center	101	7.0	6.7	0.3	0.1	6.5	4
Σ	115	14.1	13.7	0.4	0.1	7.1	3
(II) *Beggiatoa*							
Dense mats (100% coverage)	30	2.6	2.3	0.3	0.4	3.2	12
Patchy mats (<35% coverage)	55	1.7	1.5	0.2	0.3	3.1	12
Σ	85	4.3	3.8	0.5	0.7	6.3	12
(III) Gray mats (25% of hummocky area)							
Mat-covered area	80	2.8	2.0	0.9	3.5	4.8	32
Around mats	60	17.0	17.0	nd†	nd†	3.4	nd†
Σ	140	19.8	19.0	>0.9	>3.5	8.2	nd†
(IV) Siboglinid tubeworms (75% of hummocky area)							
Siboglinid assemblages	410	9.1	0.6	8.5	23.1	66.0	93
Entire HMMV ecosystem‡	750	47.3	37.1	10.3	27.3	87.6	22

* SR = sulfate reduction.
† nd = not determined.
‡ HMMV = Håkon Mosby Mud Volcano.

consumption rates with focused, gaseous methane release, and efficiency in the range of 1–24% was suggested for the different habitats (Niemann et al. 2006). Here we have calculated habitat-specific efficiencies in the removal of methane based on the ratio between aerobic or anaerobic microbial methane consumption and the total dissolved methane fluxes (Table 3).

In the center (I) of the HMMV, $> 14 \times 10^3$ mol methane d^{-1} are released (Table 4) and $< 3\%$ of the total methane flux is consumed, mostly by aerobic oxidation of methane. This low ratio is caused by shallow penetration depth of oxygen and sulfate, which restricts aerobic and anaerobic methane oxidation to a small horizon at the sediment surface (de Beer et al. 2006; Niemann et al. 2006; Lösekann et al. 2007). In the *Beggiatoa* mats (II), despite lower fluid flow velocities, the diffusion of electron acceptors into the sediment is still limited, resulting also in low consumption of the total dissolved flux of 12%, mostly by AOM (Table 3). In the gray mats (III), fluid flow is nearly absent, increasing the penetration of sulfate. As a result, more of the methane flux (32%) is consumed in the seafloor compared to the center (I) or the *Beggiatoa* mats (II). In the siboglinid tubeworm (IV) habitat, the low methane emission rate (Table 3) suggests low upward fluid flow velocities. However, with 93% turnover, the tubeworm communities are also the most efficient filter against methane, due to the bio-irrigation of the sediments by the tubeworms (Sommer et al. 2009).

For the entire geostructure, 22% of the total diffuse methane flux (47×10^3 mol d^{-1}) was removed already within the seafloor based on our measurements of methane oxidation (10×10^3 mol d^{-1}; Table 4). Taking total sulfide production (sulfate reduction; 27×10^3 mol d^{-1}) rates into account, assuming that the SR is mainly fueled by AOM at the HMMV, the efficiency increases to 58%. Including also the focused, gaseous methane efflux, which was previously found to be in the same range (Niemann et al. 2006; Sauter et al. 2006), the microbial filter for methane is only 10–26%. However, assuming that oxygen is the ultimate sink for all methane-derived reduced energy, including the previously overlooked contribution of aerobic oxidation of methane in the mats and the recycling of chemosynthetic biomass in the food web (Van Gaever et al. 2009*a*; Lichtschlag et al. 2010), the benthic filter would account for almost all of the total diffuse methane flux, indicating that a substantial proportion of biogeochemical processes at seeps is occurring in the bottom-water–sediment boundary layer.

In conclusion, by targeted in situ quantification of oxygen, methane, and sulfide fluxes during several expeditions to the HMMV, we could develop a spatial budget for the four main habitats on a scale ranging from 10 m to 1000 m. The dissolved methane efflux at HMMV of up to 777 mmol m^{-2} d^{-1} (mud volcano center) is so far the highest emission recorded in cold seep habitats, indicating also the importance of diffuse fluxes for budget estimates. For the entire mud volcano, the total dissolved methane efflux sums up to 14×10^6 mol yr^{-1}, compared to a gaseous emission of $8–35 \times 10^6$ mol yr^{-1}, as previously estimated (Sauter et al. 2006). Although not statistically significant in all cases, the distribution of the different

habitats of the HMMV was related, with temperature gradients ranging from 46°C m^{-1} to 1°C m^{-1}. The temperature gradients were closely correlated to the efflux of dissolved methane to the hydrosphere, declining from the warm, northern center of the HMMV toward the outer rim populated by thiotrophic tubeworms. The decrease in methane emission was associated with an increase in the mean oxygen consumption, reflecting the increasing efficiency of chemosynthetic organisms to consume methane and sulfide at decreasing upward fluid flow conditions. Within and between the main habitats we recorded differences in methane, sulfide, and oxygen fluxes of an order of magnitude, indicating the relevance of targeted spatial sampling in cold seep ecosystems.

At the high fluid flow rates dominating the HMMV, the microbial efficiency in consuming methane in the seabed was strongly limited, accounting for only 22% of the diffuse methane emission. However, previously overlooked processes at the sediment–water interface, including the aerobic oxidation of methane, and recycling of chemosynthetic production in the Beggiatoa mats, could contribute considerably to the methane filter as suggested by in situ total oxygen consumption measurements with benthic chambers.

Acknowledgments

We thank the ship and science crews of R/V *L'Atalante*, *Pourquoi pas?*, and *Polarstern*, as well as the teams of the ROVs *Victor6000* (IFREMER), and *Quest4000* (MARUM) for their help with work at sea. We are grateful for the technical support from Martina Alisch, Viola Beier, Imke Busse, Gabrielle Schüßler, Gabriele Eickert, and Tomas Wilkop. Thanks to Volker Asendorf, Patrick Meyer, Axel Nordhausen, and Marc Viehweger for construction and maintenance of in situ devices, to our colleagues Anna Lichtschlag and Dirk de Beer for many discussions, and to Stefanie Grünke and Angela Schäfer for helping us with the Economic and Social Research Institute geographic information system program. We also thank Mary I. Scranton and two anonymous reviewers for their helpful comments. This study was performed in the framework of the ''Geotechnologien'' project MUMM I (Methane in the Geo/Bio-System - Turnover, Metabolism and Microbes) and MUMM II (03G0608C) funded by the German Ministry of Education and Research and by the German Research Foundation. It also contributed to the European Union's 6th Framework Research Program 'Hotspot Ecosystems Research on the Margins of European Seas' (GOCE-CT-2005-511234-1) and the MARUM Center for Marine Environmental Sciences (University Bremen). This is GEOTECH publication 1680.

References

Boetius, A., and others. 2000. A marine microbial consortium apparently mediating anaerobic oxidation of methane. Nature **407:** 623–626, doi:10.1038/35036572

Cordes, E. E., D. C. Bergquist, K. Shea, and C. R. Fisher. 2003. Hydrogen sulphide demand of long-lived vestimentiferan tube worm aggregations modifies the chemical environment at deep-sea hydrocarbon seeps. Ecol. Lett. **6:** 212–219, doi:10.1046/j.1461-0248.2003.00415.x

Dattagupta, S., M. A. Arthur, and C. R. Fisher. 2008. Modification of sediment geochemistry by the hydrocarbon seep tubeworm *Lamellibrachia luymesi*: A combined empirical and modeling approach. Geochim. Cosmochim. Acta **72:** 2298–2315, doi:10.1016/j.gca.2008.02.016

———, L. L. Miles, M. S. Barnabei, and C. R. Fisher. 2006. The hydrocarbon seep tubeworm *Lamellibrachia luymesi* primarily eliminates sulfate and hydrogen ions across its roots to conserve energy and ensure sulfide supply. J. Exp. Biol. **209:** 3795–3805, doi:10.1242/jeb.02413

de Beer, D., and others. 2006. In situ fluxes and zonation of microbial activity in surface sediments of the Håkon Mosby mud volcano. Limnol. Oceanogr. **51:** 1315–1331, doi:10.4319/lo.2006.51.3.1315

Dimitrov, L. I. 2002. Mud volcanoes—the most important pathway for degassing deeply buried sediments. Earth-Sci. Rev. **59:** 49–76, doi:10.1016/S0012-8252(02)00069-7

Elvert, M., and H. Niemann. 2008. Occurrence of unusual steroids and hopanoids derived from aerobic methanotrophs at an active marine mud volcano. Org. Geochem. **39:** 167–177, doi:10.1016/j.orggeochem.2007.11.006

Feseker, T., J. P. Foucher, and F. Harmegnies. 2008. Fluid flow or mud eruptions? Sediment temperature distributions on Håkon Mosby mud volcano, SW Barents Sea slope. Mar. Geol. **247:** 194–207, doi:10.1016/j.margeo.2007.09.005

Foucher, J. P., and others. 2009. Structure and drivers of cold seep ecosystems. Oceanography **22:** 92–109.

Glud, R. N. 2008. Oxygen dynamics of marine sediments. Mar. Biol. Res. **4:** 243–289, doi:10.1080/17451000801888726

———, J. K. Gundersen, H. Røy, and B. B. Jørgensen. 2003. Seasonal dynamics of benthic O_2 uptake in a semi-enclosed bay: Importance of diffusion and faunal activity. Limnol. Oceanogr. **48:** 1265–1276, doi:10.4319/lo.2003.48.3.1265

Jerosch, K., M. Schlüter, J. P. Foucher, A. G. Allais, M. Klages, and C. Edy. 2007. Spatial distribution of mud flows, chemoautotrophic communities, and biogeochemical habitats at Håkon Mosby Mud Volcano. Mar. Geol. **243:** 1–17, doi:10.1016/j.margeo.2007.03.010

Jørgensen, B. B. 1978. A comparison of methods for the quantification of bacterial sulfate reduction in coastal marine sediments I. Measurements with radiotracer techniques. Geomicrobiol. J. **1:** 11–27, doi:10.1080/01490457809377721

———, and A. Boetius. 2007. Feast and famine—microbial life in the deep-sea bed. Nat. Rev. Microbiol. **5:** 770–781, doi:10.1038/nrmicro1745

Kallmeyer, J., T. G. Ferdelman, A. Weber, H. Fossing, and B. B. Jørgensen. 2004. A cold chromium distillation procedure for radiolabeled sulfide applied to sulfate reduction measurements. Limnol. Oceanogr.: Methods **2:** 171–180.

Knittel, K., and A. Boetius. 2009. Anaerobic oxidation of methane: Progress with unknown process. Annu. Rev. Microbiol. **63:** 311–334, doi:10.1146/annurev.micro.61.080706.093130

Kopf, A. J. 2002. Significance of mud volcanism. Rev. Geophys. **40**(2): 1–45, doi:10.1029/2000RG000093

Kvenvolden, K. A., and B. W. Rogers. 2005. Gaia's breath—global methane exhalations. Mar. Petrol. Geol. **22:** 579–590, doi:10.1016/j.marpetgeo.2004.08.004

Lichtschlag, A., J. Felden, V. Brüchert, A. Boetius, and D. de Beer. 2010. Geochemical processes and chemosynthetic primary production in different thiotrophic mats of the Håkon Mosby Mud Volcano (Barents Sea). Limnol. Oceanogr. **55:** 931–949.

Linke, P., E. Suess, M. Torres, V. Martens, W. D. Rugh, W. Ziebis, and L. D. Kulm. 1994. In situ measurement of fluid-flow from cold seeps at active continental margins. Deep-Sea Res. Part I **41:** 721–739, doi:10.1016/0967-0637(94)90051-5

———, K. Wallmann, E. Suess, C. Hensen, and G. Rehder. 2005. In situ benthic fluxes from an intermittently active mud volcano at the Costa Rica convergent margin. Earth Planet. Sci. Lett. **235:** 79–95, doi:10.1016/j.epsl.2005.03.009

Lösekann, T., K. Knittel, T. Nadalig, B. Fuchs, H. Niemann, A. Boetius, and R. Amann. 2007. Diversity and abundance of aerobic and anaerobic methane oxidizers at the Håkon Mosby mud volcano, Barents Sea. Appl. Environ. Microbiol. **73:** 3348–3362, doi:10.1128/AEM.00016-07

———, A. Robador, H. Niemann, K. Knittel, A. Boetius, and N. Dubilier. 2008. Endosymbioses between bacteria and deep-sea siboglinid tubeworms from an Arctic Cold Seep (Håkon Mosby mud volcano, Barents Sea). Environ. Microbiol. **10:** 3237–3254, doi:10.1111/j.1462-2920.2008.01712.x

Milkov, A. V., R. Sassen, T. V. Apanasovich, and F. G. Dadashev. 2003. Global gas flux from mud volcanoes: A significant source of fossil methane in the atmosphere and the ocean. Geophys. Res. Lett. **30**, doi:10.1029/2002GL016358

———, P. R. Vogt, K. Crane, A. Y. Lein, R. Sassen, and G. A. Cherkashev. 2004. Geological, geochemical, and microbial processes at the hydrate-bearing Håkon Mosby mud volcano: A review. Chem. Geol. **205:** 347–366, doi:10.1016/j.chemgeo.2003.12.030

Naganuma, T., H. E. Elsaied, D. Hoshii, and H. Kimura. 2005. Bacterial endosymbioses of gutless tube-dwelling worms in non-hydrothermal vent habitats. Mar. Biotech. **7:** 416–428, doi:10.1007/s10126-004-5089-3

———, and others. 1999. Sea-floor fissures, biological communities and sediment fatty acids of the Northern Okushiri Ridge, Japan Sea: Implications for possible methane seepage. Isl. Arc. **8:** 232–244, doi:10.1046/j.1440-1738.1999.00234.x

Naguib, M. 1976. Stoichiometry of methane oxidation in the methane-oxidizing strain M 102 under the influence of various CH_4/O_2 mixtures. Z. Allg. Mikrobiol. **16:** 437–444, doi:10.1002/jobm.3630160604

Niemann, H., and others. 2006. Novel microbial communities of the Håkon Mosby mud volcano and their role as a methane sink. Nature **443:** 854–858, doi:10.1038/nature05227

Olu, K., S. Lance, M. Sibuet, P. Henry, A. Fialamedioni, and A. Dinet. 1997. Cold seep communities as indicators of fluid expulsion patterns through mud volcanoes seaward of the Barbados accretionary prism. Deep-Sea Res. Part I **44:** 811–841, doi:10.1016/S0967-0637(96)00123-9

Olu-Le Roy, K., and others. 2004. Cold seep communities in the deep eastern Mediterranean Sea: Composition, symbiosis and spatial distribution on mud volcanoes. Deep-Sea Res. Part I **51:** 1915–1936, doi:10.1016/j.dsr.2004.07.004

Pérez-Garcia, C., T. Feseker, J. Mienert, and C. Berndt. 2009. The Håkon Mosby mud volcano: 330,000 years of focused fluid flow activity at the SW Barents Sea slope. Mar. Geol. **262:** 105–115, doi:10.1016/j.margeo.2009.03.022

Reeburgh, W. S. 2007. Oceanic methane biogeochemistry. Chem. Rev. **107:** 486–513, doi:10.1021/cr050362v

Røy, H., M. Hüttel, and B. B. Jørgensen. 2002. The role of small-scale sediment topography for oxygen flux across the diffusive boundary layer. Limnol. Oceanogr. **47:** 837–847, doi:10.4319/lo.2002.47.3.0837

Sauter, E. J., and others. 2006. Methane discharge from a deep-sea submarine mud volcano into the upper water column by gas hydrate-coated methane bubbles. Earth Planet. Sci. Lett. **243:** 354–365, doi:10.1016/j.epsl.2006.01.041

———, M. Schluter, and E. Suess. 2001. Organic carbon flux and remineralization in surface sediments from the northern North Atlantic derived from pore-water oxygen microprofiles. Deep-Sea Res. Part I **48:** 529–553, doi:10.1016/S0967-0637(00)00061-3

Shirayama, Y. 1992. Respiration rates of bathyal meiobenthos collected using a deep-sea submersible Shinkai-2000. Deep-Sea Res. Part I **39:** 781–788.

Sibuet, M., and K. Olu. 1998. Biogeography, biodiversity and fluid dependence of deep-sea cold-seep communities at active and passive margins. Deep-Sea Res. Part II **45:** 517–567, doi:10.1016/S0967-0645(97)00074-X

Smirnov, R. V. 2000. Two new species of Pogonophora from the arctic mud volcano off northwestern Norway. Sarsia **85:** 141–150.

Sommer, S., P. Linke, O. Pfannkuche, H. Niemann, and T. Treude. In press. Benthic respiration in a seep habitat dominated by dense beds of ampharetid polychaetes at the Hikrangi Margin (New Zealand). Mar. Geol.

———, and others. 2009. Seabed methane emission and the habitat of frenulate tubeworms on the Captain Arutyunov mud volcano (Gulf of Cadiz). Mar. Ecol.-Prog. Ser. **382:** 69–86, doi:10.3354/meps07956

———, and ———. 2006. Efficiency of the benthic filter: Biological control of the emission of dissolved methane from sediments containing shallow gas hydrates at Hydrate Ridge. Glob. Biogeochem. Cycles **20**, doi:10.1029/2004GB002389

———, and ———. 1999. Gas hydrate destabilization: Enhanced dewatering, benthic material turnover and large methane plumes at the Cascadia convergent margin. Earth Planet. Sci. Lett. **170:** 1–15, doi:10.1016/S0012-821X(99)00092-8

Teske, A., and D. C. Nelson. 2006. The genera *Beggiatoa* and *Thioploca*, p. 784–810. *In* M. Dworkin, S. Falkow, S. Rosenberg, K.-H. Schleifer and E. Stackebrandt [eds.], The prokaryotes, v. 6. Proteobacteria: Gamma subclass. Springer.

Torres, M. E., and others. 2002. Fluid and chemical fluxes in and out of sediments hosting methane hydrate deposits on Hydrate Ridge, OR, I: Hydrological provinces. Earth Planet. Sci. Lett. **201:** 525–540, doi:10.1016/S0012-821X(02)00733-1

Treude, T., A. Boetius, K. Knittel, K. Wallmann, and B. B. Jørgensen. 2003. Anaerobic oxidation of methane above gas hydrates at Hydrate Ridge, NE Pacific Ocean. Mar. Ecol.-Prog. Ser. **264:** 1–14, doi:10.3354/meps264001

Van Gaever, S., L. Moodley, D. de Beer, and A. Vanreusel. 2006. Meiobenthos at the Arctic Håkon Mosby mud volcano, with a parental-caring nematode thriving in sulphide-rich sediments. Mar. Ecol.-Prog. Ser. **321:** 143–155, doi:10.3354/meps321143

———, ———, F. Pasotti, M. Houtekamer, J. J. Middelburg, R. Danovaro, and A. Vanreusel. 2009*a*. Trophic specialisation of metazoan meiofauna at the Håkon Mosby mud volcano: Fatty acid biomarker isotope evidence. Mar. Biol. **156:** 1289–1296, doi:10.1007/s00227-009-1170-9

———, K. Olu, S. Derycke, and A. Vanreusel. 2009*b*. Metazoan meiofaunal communities at cold seeps along the Norwegian margin: Influence of habitat heterogeneity and evidence for connection with shallow-water habitats. Deep-Sea Res. Part I **56:** 772–785, doi:10.1016/j.dsr.2008.12.015

Wenzhöfer, F., and R. N. Glud. 2002. Benthic carbon mineralization in the Atlantic: A synthesis based on *in situ* data from the last decade. Deep-Sea Res. Part I **49:** 1255–1279, doi:10.1016/S0967-0637(02)00025-0

Associate editor: Mary I. Scranton

Received: 07 October 2009
Accepted: 08 July 2010
Amended: 13 July 2010